Structure and Sodium Ion Dynamics in Sodium Strontium Silicate Investigated by Multinuclear Solid-State NMR

Kenneth K. Inglis,[1] John P. Corley,[1] Pierre Florian,[2] Jordi Cabana,[3] Ryan D. Bayliss[*,3], Frédéric Blanc,*[*,1,4]

[1] Department of Chemistry, University of Liverpool, Crown Street, Liverpool, L69 7ZD, United Kingdom;

[2] Conditions Extrême et Matériaux: Haute Température and Irradiation, CNRS-UPR 3079, 1 d Avenue de la Recherche Scientifique, 45071 Orléans, Cedex 2, France;

[3] Department of Chemistry, University of Illinois at Chicago, 845 West Taylor Street, Chicago, Illinois, 60607, USA;

[4] Stephenson Institute for Renewable Energy, University of Liverpool, Crown Street, Liverpool, L69 7ZD, United Kingdom.

* To whom correspondence should be addressed (R.D.B. and F.B.).

E-mail: rbayliss@uic.edu & frederic.blanc@liverpool.ac.uk

Abstract

The high oxide ion conductivity of the proposed sodium strontium silicate ion conductors $Sr_{0.55}Na_{0.45}SiO_{2.775}$ (> 10^{-2} $S.cm^{-1}$ at 525 °C) and its unusual alkali metal substitution strategy have been extensively questioned in the literature. Here, we present a comprehensive understanding of the structure of this material using a combination of XRD and multinuclear ^{17}O, ^{23}Na and ^{29}Si solid-state NMR spectroscopy data and a detailed investigation of the Na ion dynamics by high temperature ^{23}Na NMR line shape analysis and relaxation rates measurements. Both ^{23}Na and ^{29}Si NMR spectra demonstrate the absence of Na doping in strontium silicate $SrSiO_3$ and the presence of an amorphous phase identified as $Na_2O{\cdot}2SiO_2$ glass as the Na-containing product. Devitrification at 800 °C yields crystallisation of the $Na_2O{\cdot}2SiO_2$ glass into the known crystalline α-$Na_2Si_2O_5$ phase which was positively identified by its XRD pattern and the extensive and clear ^{17}O, ^{23}Na and ^{29}Si NMR fingerprints. High temperature ^{23}Na NMR reveals that the Na ions are mobile in the $Na_2O{\cdot}2SiO_2$ amorphous component below its glass transition temperature (~ 450 °C). In contrast, ^{23}Na NMR data obtained on the crystalline α-$Na_2Si_2O_5$ shows limited Na dynamics below ~ 650 °C and this result explains the large discrepancy in the conductivity observed in the literature which strongly depends on the thermal history of the $Sr_{0.55}Na_{0.45}SiO_{2.775}$ material. These insights demonstrate that the high conductivity observed in $Sr_{0.55}Na_{0.45}SiO_{2.775}$ are due to Na conduction in the $Na_2O{\cdot}2SiO_2$ glass and this motivates the quest for the discovery of low temperature fast ion conductors in non-crystalline solids.

Introduction

Strontium silicate $SrSiO_3$ and alkali metal (A site aliovalent substituents) solid solutions were recently investigated as potential intermediate temperature Solid Oxide Fuel Cell (SOFC) electrolytes. Initial reports by Singh and Goodenough proposed these materials as a new family of crystal structures able to permit rapid oxygen ion vacancy conductivity, values in excess of those previously reported in the classic fluorite and perovskite type oxides.[1,2] These newly proposed superior oxide ion conductors have been reported to possess oxide ion conductivities as high as 1.04 x 10^{-2} S.cm^{-1} at 625 °C in the $Sr_{0.8}K_{0.2}Si_{0.5}Ge_{0.5}O_{2.9}$ material which initiated a surge of interest in these new phases.[1] More impressively, higher conductivity was reported in the Na analogues with the highest total conductivity of 1.79 x 10^{-2} S.cm^{-1} at 550 °C reported in the $Sr_{0.55}Na_{0.45}SiO_{2.775}$ composition.[2] The extraordinarily high values of oxide ion conductivity reported for these phases placed them at a level competitive with the state-of-the-art oxide ion conducting ceramics currently used with significant room left for further development through chemical and microstructural optimisation.

The oxygen vacancies proposed in these structures, which were assumed as the mobile defect responsible for the high level of conductivity observed, represented a new concept for designing oxide ion conducting electrolytes. Firstly, alkali metals are typically avoided in high temperature oxide ion conductors due to their ability to be highly mobile at low temperatures in solid state materials such as the well-known Garnets.[3] However, it has been demonstrated that Na containing oxide ion electrolytes can exist and in which the oxide ion is responsible for the high levels of conductivity.[4] Secondly, oxygen vacancies on SiO_4 tetrahedra are seldom observed in the solid state, though in this instance it was postulated that the vacancies would stimulate the formation of bridging oxide ion located between two normal oxygen sites which could be part of the mechanism for rapid oxide ion conductivity. This mechanism was supported by a ^{29}Si solid state Nuclear Magnetic Resonance (NMR) study by Kuang and Wu *et al.*[5]

confirming the existence of a Si signal indicating breaking of the Si_3O_9 rings into Si_3O_8 chains, proposing the formation of linked tetrahedral Si in the rings. However, a high resolution powder neutron diffraction investigation suggested that whilst they observed single phase materials with the chemical composition as nominally written, they did not observe interstitial oxygen ion formation in the Fourier nuclear density difference maps from Rietveld refinements but rather oxygen vacancies in the planar oxygen sites of the corner sharing tetrahedral units of Si_3O_9.[6] Finally, the continuous increase reported in total conductivity as a function of alkali ion concentration absent of any obvious dopant defect interactions was very surprising as all previous oxide ion conducting systems had an optimal defect concentration for maximising total conductivity. Acceptor doped oxides typically produce a conductivity maxima at significantly lower substitutional levels than those reported in these materials,[7,8] which is associated with the formation of dimer and trimer associates,[9] but higher order clusters are possible, leading to the formation of nano-domains of secondary phases, detrimental to total conductivity.

An *in operando* demonstration of these new oxide ion conducting electrolyte materials was reported that appeared to validate these materials as superior oxide ion conducting electrolytes, with excellent fuel cell performance results.[10] The report also concluded the $Sr_{0.55}Na_{0.45}SiO_{2.775}$ materials were stable over the oxygen partial pressure range of 10^{-30} – 1 atm, preventing the deleterious effects of electronic defect contributions to the electrolyte.

In an effort to confirm the remarkable results published originally,[1,2] Bayliss *et al*[11] attempted to replicate the study and furthermore add direct confirmation of the defect responsible for conductivity, through measurements of the oxide ion mass transport. Through detailed analysis of the structural, electrochemical and mass transport properties obtained, it was proposed that both $Sr_{0.8}K_{0.2}Si_{0.5}Ge_{0.5}O_{2.9}$, and by implication of the results the $Sr_{0.55}Na_{0.45}SiO_{2.775}$ materials were in fact not single phase materials but rather biphasic mixes consisting of crystalline $SrSiO_3$ and some form of amorphous glass, postulated to be potassium digerminate

$K_2O{\cdot}2GeO_2$ or sodium disilicate $Na_2O{\cdot}2SiO_2$ glass, with the latter being responsible for the high total conductivity previously reported and the mobile defect most likely to be the alkali ion Na^+ or K^+.

The structurally analogous $Sr_{1-x}Na_xSiO_{3-x/2}$ ($0 < x \leq 0.45$) family also proposed by Singh and Goodenough[2] was shown experimentally to exhibit similar behaviour to the $Sr_{0.8}K_{0.2}Si_{0.5}Ge_{0.5}O_{2.9}$ materials by Evans *et al*[12] and Bayliss *et al*.[13] Furthermore, the latter study theoretically demonstrated the high energetic costs of anion defect formation in the $Sr_{1-x}Na_xSiO_{3-x}$ composition, suggesting their formation as unlikely.[13] Further experimental work by Tealdi *et al.*[14], Lossila *et al.*[15], Huang *et al.*,[16,17] ourselves,[18] and *ab initio* molecular dynamics simulation,[19] have since suggested this behaviour is true across all analogous structures, both K and Na proposed solid solutions.

The mobility of Na^+ has been directly probed through the use of variable temperature ^{23}Na NMR and spin–lattice relaxation times in the laboratory frame (T_1) measurements in $Sr_{0.55}Na_{0.45}SiO_{2.775}$[18] and $Sr_{0.6}Na_{0.4}SiO_{2.8}$[20] showing conclusively that the Na^+ ions are highly mobile.[20] The ^{23}Na NMR spectra showed a single broad asymmetric peak which narrows down as the temperature is increased to 350 °C,[20] as expected for Na^+ diffusion in a distribution of local environments such as those found in amorphous compounds such as $Na_2O{\cdot}2SiO_2$, confirming the absence of Na doping in $SrSiO_3$ and that Na was present only in the amorphous phase in any significant proportion. Additionally, a decrease in T_1 with increasing temperature was observed, confirming both the Na^+ are mobile and their mobility is thermally activated.

It is well known that glasses can crystallise when heated above their glass transition temperature T_g[21] at a speed which depends upon the viscosity of this super-cooled liquid. For $Na_2O{\cdot}2SiO_2$ (T_g = 450 °C)[22], previous *in situ* high-temperature NMR experiments have shown that the super-cooled liquid is stable over the course of an NMR experiment up to approximately 700 °C.[23,24] Both studies have evidenced exchange between the Q^n species (n = 2, 3 and 4) in the

super-cooled liquid by ^{29}Si NMR while Liu *et al.*[23] additionally showed a ^{23}Na T_1 minimum around 530 °C and an associated activation energy of 67 ± 5 kJ.mol^{-1}, close to measured values for tracer diffusion or electrical conductivity in melts (55 to 75 kJ.mol^{-1}).[25–30] The recent *in situ* ^{23}Na NMR investigation by Evans *et al.*[20] performed on the mixed $Sr_{0.60}Na_{0.40}SiO_{2.80}$ composition up to 350 °C yields an activation energy (23 kJ.mol^{-1}) close to the 31 kJ.mol^{-1} value obtained by impedance spectroscopy.[10] This decrease in activation energy is somewhat contradictory with the well described "mixed alkali effect"[31] and an opposite trend has been observed for the mixed Na/K disilicate system,[23] hence the importance to rationalize the high temperature ^{23}Na NMR behaviour.

More recently, Hu *et al.*[32] performed a multinuclear solid state NMR investigation in an attempt to determine the structure, chemical composition and ion dynamics of all species in various levels of Na substituted $SrSiO_3$. Interestingly and contrary to most recent work[11–14,18,20] the authors suggest up to 10 mol% Na substitution is possible on the Sr site in the $SrSiO_3$ lattice, with concentrations above this value causing phase separation to occur and leading to the formation of, to the best of our knowledge, a previously unreported amorphous β-$Na_2Si_2O_5$ phase. The proposed phase separation on increasing Na concentration above 10 mol% is unusual and this amongst other issues are addressed in further detail during the main body of this work.

$Na_2Si_2O_5$ has a complex polymorphism[33] with a melting point at 874 °C,[34] and completely devitrifies to form the crystalline α-$Na_2Si_2O_5$ phase above 650 °C for which the XRD patterns[35] and all ^{17}O,[36,37] ^{23}Na,[38–40] ^{29}Si[38,41,42] solid state NMR spectra[43] are known and are uniquely characteristic of this phase, therefore providing an additional pathway for phase identification whether crystalline or amorphous. Additionally, a large range of ionic conductivities have been reported in the literature for $Sr_{0.55}Na_{0.45}SiO_{2.775}$ from ac impedance data[2,10,14,16] and may arise from this devitrification process and the thermal history of the sample

since it was recently postulated by *ab initio* molecular dynamics simulation that while $Na_2O{\cdot}2SiO_2$ glass is a good Na^+ conductor, crystalline $Na_2Si_2O_5$ is an insulator.[19]

In this work, we focus on a complete structural and Na^+ ion dynamics solid state NMR study of the proposed sodium strontium silicate fast ion conductors of nominal composition $Sr_{0.55}Na_{0.45}SiO_{2.775}$ over a wide temperature range that follows our initial investigations.[11,13] The unique capability of NMR to probe, in both amorphous and crystalline materials, the local structure and ion dynamics in fast ion conductors[44,45] permits to explain the previous experimental results described above that have been the subject of debates in the literature.[1,2,5,6,10–20,32] Upon devitrification of $Sr_{0.55}Na_{0.45}SiO_{2.775}$ at 800 °C, the amorphous $Na_2O{\cdot}2SiO_2$ glassy phase not observed by XRD forms crystalline α-$Na_2Si_2O_5$ as evidence by the XRD data and ^{17}O, ^{23}Na and ^{29}Si NMR spectra fingerprints. Extensive variable temperature ^{23}Na NMR data including line shape analysis, spin–lattice relaxation rates in the laboratory frame (T_1^{-1}) and/or in the rotating frame ($T_{1\rho}^{-1}$) evolution as a function of temperature provides compelling evidence for the fast and slow Na dynamics in as prepared and devitrified $Sr_{0.55}Na_{0.45}SiO_{2.775}$, respectively. These results highlight the fast Na^+ transport in amorphous $Na_2O{\cdot}2SiO_2$ glass and its absence in α-$Na_2Si_2O_5$, respectively, and highlight potential for the design of non-crystalline solid state fast ion conductors.

Materials and Methods

Light blue $Sr_{0.55}Na_{0.45}SiO_{2.775}$ was prepared by solid state synthesis from $SrCO_3$ (Sigma-Aldrich, > 99.9 %), Na_2CO_3 (Sigma-Aldrich, > 99.9999 %) and SiO_2 (Sigma-Aldrich, > 99.9 %) following a literature procedure (thereafter called as prepared).[2] The same sample was used throughout this work and previous studies by our groups,[13] removing any ambiguity in sample composition. The starting materials were mixed in a stoichiometric amount using a mortar and pestle and then heated at 1050 °C for 20 h in air in an Al_2O_3 crucible, with heating and cooling

rates of 5 °C.min^{-1}. Devitrification of $Sr_{0.55}Na_{0.45}SiO_{2.775}$ was performed by holding the as prepared sample at 800 °C for 4 h (heating and cooling rates of 5 °C.min^{-1}) in air using a Al_2O_3 crucible. Oxygen ^{17}O enrichment was performed by heating the devitrified $Sr_{0.55}Na_{0.45}SiO_{2.775}$ sample in a Quartz tube under 60 % ^{17}O enriched $^{17}O_2$ gas (Sigma-Aldrich, used as received) at 750 °C in a tube furnace for 24 h (heating and cooling rates of 5 °C.min^{-1}).

XRD patterns were obtained on a PANalytical X'Pert Pro diffractometer using the CoKα radiation of wavelength 1.79 Å. A layer of powder was put on a thin layer of grease spread onto the surface of a glass disk which was used as the sample holder. Rietveld refinements of the data were performed using EXPGUI[46] and GSAS.[47] Crystallographic information files (CIF) were used as starting models for the structural refinements, obtained from the Inorganic Crystal Structure Database (ICSD). During the refinements, the background, lattice cell parameters, zero point error and atomic positions for Sr and Si were refined. The atomic displacement parameters (ADP) were fixed as equivalent for each atomic species and allowed to refine.

^{17}O, ^{23}Na and ^{29}Si solid state NMR experiments were performed on a 9.4 T Bruker Avance III HD 400 MHz spectrometer equipped with a Bruker 4 mm HXY Magic Angle Spinning (MAS) probe (in double resonance mode) or a Bruker 4 mm HX MAS high temperature probe (for variable temperature experiments). Additional high temperature ^{23}Na NMR experiments above 360 °C were carried out on a 9.4 T Bruker Avance spectrometer using a single channel static liquid state NMR probe and a homemade CO_2 laser (λ = 10.6 μm, 250 W) heating system developed in Orléans (CNRS – CEMHTI).[48,49] The sample is placed inside a boron nitride BN crucible (chemically inert to $Sr_{0.55}Na_{0.45}SiO_{2.775}$ at high temperature, see XRD data and text) and is heated by 2 laser beams passing axially through the NMR probe, irradiating the top and bottom of the BN crucible to ensure temperature homogeneity. A flow of air is used for thermal shielding and cooling of the radio frequency coil and an Ar stream prevents oxidation of the BN crucible at high temperature. One dimensional ^{17}O NMR spectra were

obtained at a MAS frequency of 13 kHz with a rotor synchronised Hahn echo 90 – τ – 180 – τ – acq sequence with a delay τ of 77 μs (1 rotor period) and using solid 90 degree pulse of 1.2 μs at a rf field amplitude of 70 kHz. One dimensional ^{23}Na static NMR spectra were also obtained with an echo sequence (τ = 30 μs). ^{23}Na MAS NMR spectra were obtained at a MAS frequency of 10 kHz with a one pulse sequence. All ^{23}Na 90 degree pulse were of 1.5 μs at a rf field amplitude of 83 kHz on the MAS probe and of 13 μs at a rf field amplitude of 9.6 kHz on the static laser probe (unless otherwise specified). The one dimensional ^{29}Si NMR spectra were obtained at a MAS frequency of 10 kHz with a one pulse sequence using 90 degree pulse of 5 μs at a rf field amplitude of 50 kHz.

Spin–lattice relaxation times T_1 in the laboratory frame were recorded under static conditions and at $\nu_0(^{23}Na)$ = 105.8 MHz with a saturation recovery pulse sequence, and were fitted to a single stretched exponential of the form $1 - \exp[-(\tau/T_1)^{\alpha}]$ (where τ are variable delays and α the stretched exponential factor). For the as prepared $Sr_{0.55}Na_{0.45}SiO_{2.775}$ sample due to the onset of crystallization of the $Na_2O{\cdot}2SiO_2$ glass into crystalline α-$Na_2Si_2O_5$ across the crystallisation phase transition temperatures T_cs (490 – 650 °C) which have very different T_1, the data were fitted with a double stretched exponential of the form $1 - \exp[-(\tau/T_{1(1)})^{\alpha}]) + 1 - \exp[-(\tau/T_{1(2)})^{\beta}]$ (where $T_{1(1)}$ and $T_{1(2)}$ are the different spin–lattice relaxation times), and follow a similar approach used previously on $Na_2O{\cdot}2SiO_2$ glass around 635 – 699 °C.[23] Spin–lattice relaxation times $T_{1\rho}$ in the rotating frame were obtained under static condition with a spin lock sequence at frequencies of $\nu_1(^{23}Na) \approx 20$ and 35 kHz on the 4 mm HX MAS high temperature NMR probe, and at ≈ 6.7 and 9.6 kHz on the static laser probe, the data obtained fitted to a single stretched exponential. Temperature calibration of the 4 mm HX MAS high temperature NMR probe was performed using the ^{207}Pb NMR resonance of $Pb(NO_3)_2$,[50,51] the ^{63}Cu resonances of $Cu^{I}Br$ across the γ-to-β phase transition at 385 °C and of $Cu^{I}I$ across the γ-to-β

phase transition at 369 °C,[52,53] while temperature calibration of the static laser probe was obtained by the direct measurement of the melting points of reference samples. The sample temperatures quoted subsequently have all been corrected according to this calibration, and have an accuracy of approximately ± 10 °C (between room temperature and 150 °C), ± 20 °C (between 150 °C and 360 °C) and ± 15 °C (above 360 °C on the static laser probe).

High field ^{17}O and ^{23}Na solid state NMR experiments were performed on a 20 T Bruker Avance II 850 MHz spectrometer using Bruker 3.2 mm HXY MAS probe (in double resonance mode) and Bruker 2.5 mm HX MAS probe, respectively. The one dimensional ^{17}O NMR spectrum was obtained at a MAS frequency of 22 kHz with a rotor synchronised Hahn echo sequence (1 rotor period) using solid 90° degree pulse of 1 μs at a rf field amplitude of 83 kHz. One dimensional ^{23}Na NMR spectra were obtained at a MAS frequency of 30 kHz with a one pulse sequence using solid 90 degree pulse of 1.25 μs at a rf field amplitude of 100 kHz.

All ^{17}O, ^{23}Na and ^{29}Si shifts were externally referenced to H_2O, 1 M NaCl in H_2O and $Si(CH_4)_3$ at 0 ppm, respectively.

Results and Discussions

Phase identification with XRD

A sample of nominal composition $Sr_{0.55}Na_{0.45}SiO_{2.775}$ was obtained by solid state synthesis using a known procedure[2] involving heating at 1050 °C in air (cooling and heating rates of 5 °C.min^{-1}). The XRD pattern of $Sr_{0.55}Na_{0.45}SiO_{2.775}$ (Figure 1a) was refined in space group C2/c with lattice cell parameters and atomic coordinates matching the expected ones from the previous neutron diffraction investigation[13] and crystalline α-$SrSiO_3$ (ICSD n° 59308).[54] As before, no other peaks than α-$SrSiO_3$ were observed in $Sr_{0.55}Na_{0.45}SiO_{2.775}$. However, in the devitrified $Sr_{0.55}Na_{0.45}SiO_{2.775}$ sample an additional set of reflections corresponding to α-

$Na_2Si_2O_5$ (ICSD n° 34669)[35] are clearly visible and were refined by Rietveld giving acceptable quality of fit values (low tick marks Figure 1b).

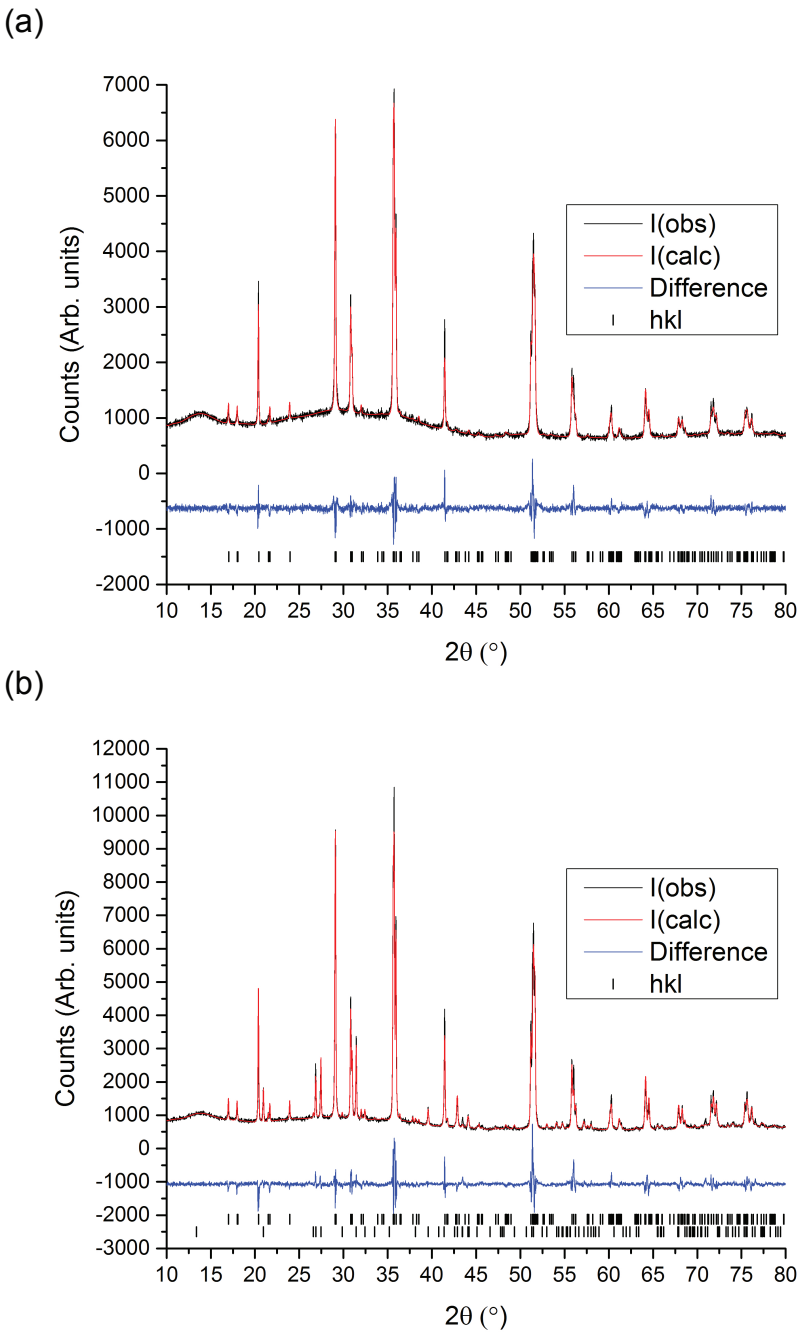

Figure 1. Rietveld refinements of XRD data of (a) $Sr_{0.55}Na_{0.45}SiO_{2.775}$ and (b) devitrified $Sr_{0.55}Na_{0.45}SiO_{2.775}$. The results clearly show that the material is two phase in nature which agrees with previous work.[12–14] The crystalline phases present are α-$SrSiO_3$ (ICSD n° 59308)[54] and α-$Na_2Si_2O_5$ (ICSD n° 34669)[35] (lower tick marks in b).

Phase identification with multinuclear ^{29}Si, ^{23}Na and ^{17}O NMR spectroscopy

The ^{29}Si NMR spectrum of $Sr_{0.55}Na_{0.45}SiO_{2.775}$ is given in Figure 2a and shows a sharp resonance at – 84.8 ppm in addition to broad signals between – 77 ppm and – 99 ppm, as observed by Evans *et al.*[12] and Tealdi *et al.*[14] The sharp line is typical of a crystalline phase (as also evidenced by the long T_1 relaxation time of ^{29}Si estimated around 60 min) and is assigned to α-$SrSiO_3$ based on its shift.[55] The broad line and its short T_1 relaxation time (0.2 s) reflect the presence of an amorphous phase identified as sodium disilicate $Na_2O{\cdot}2SiO_2$ glass by previous quantification of the XRD patterns[11] and comparison with the known ^{29}Si MAS spectrum of this $Na_2O{\cdot}2SiO_2$ glass reported by Stebbins *et al.*[56] which shows three broad and Gaussian signals resonating at – 77, – 88 and – 99 ppm and corresponding to Q^2, Q^3 and Q^4 units.

The ^{29}Si NMR spectrum of devitrified $Sr_{0.55}Na_{0.45}SiO_{2.775}$ (Figure 2b) also reveals the presence of the same sharp signal at – 84.8 ppm (α-$SrSiO_3$). However, the broad signals of $Na_2O{\cdot}2SiO_2$ glass in $Sr_{0.55}Na_{0.45}SiO_{2.775}$ have now completely disappeared and have been replaced by a sharp signal at – 94.3 ppm (with a long T_1 of approximately 100 min) assigned to crystalline α-$Na_2Si_2O_5$ phase.[38,41,42] This observation agrees well with the devitrification of $Na_2O{\cdot}2SiO_2$ glass under the heat treatment condition used (800 °C and 1 bar)[33] to devitrified $Sr_{0.55}Na_{0.45}SiO_{2.775}$ from the as prepared $Sr_{0.55}Na_{0.45}SiO_{2.775}$. A related ^{29}Si NMR spectrum of a devitrified $Sr_{0.55}Na_{0.45}SiO_{2.775}$ sample at 650 °C was previously observed,[14] although it shows the presence of three unexplained additional ^{29}Si resonances between – 87 and – 92 ppm which could actually be assigned to β-$Na_2Si_2O_5$ (two Q^3 Si environments at – 86.7 and – 88.6 ppm)[38,39] and γ-$Na_2Si_2O_5$ (one Q^3 Si environments at – 90.4 ppm),[38] two other known polymorphs of $Na_2Si_2O_5$.[33]

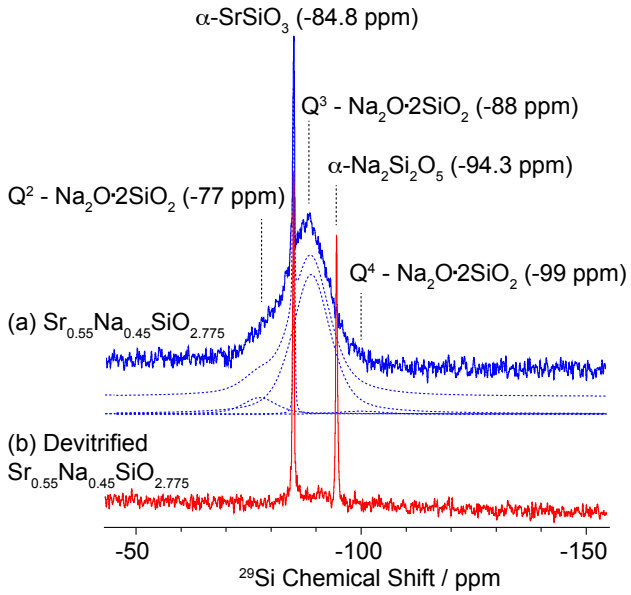

Figure 2. ^{29}Si MAS NMR spectra of (a) $Sr_{0.55}Na_{0.45}SiO_{2.775}$ and (b) devitrified $Sr_{0.55}Na_{0.45}SiO_{2.775}$ obtained at 9.4 T. Dashed lines represent line shape simulation and deconvolution of the three Q2, Q3 and Q4 units of the $Na_2O{\cdot}2SiO_2$ glass.[56]

The ^{23}Na MAS NMR spectrum (Figure 3) of $Sr_{0.55}Na_{0.45}SiO_{2.775}$ obtained at 9.4 T shows a broad line shape with a tail at low frequency, similar to $Na_2O{\cdot}2SiO_2$ glass[57] and the recent work on $Sr_{0.6}Na_{0.4}SiO_{2.8}$.[20] The tail results from a distribution of quadrupolar couplings[58] and indicates the presence of significant structural disorder and a range of Na sites (also corroborated by the short T_1 time measured of 98 ± 11 ms). All these observations are therefore in agreement with the presence of an amorphous Na-containing glass in $Sr_{0.55}Na_{0.45}SiO_{2.775}$. A MAS spectrum recorded at a higher field of 20 T yields a narrower line, as anticipated,[59] nevertheless no additional Na site is observed as is commonly observed in glasses.

In contrast to $Sr_{0.55}Na_{0.45}SiO_{2.775}$, devitrified $Sr_{0.55}Na_{0.45}SiO_{2.775}$ shows the typical ^{23}Na second order line shape of α-$Na_2Si_2O_5$[38], reinforcing that this phase is formed upon devitrification of the $Na_2O{\cdot}2SiO_2$ glass. More importantly, it also shows that Na is only present as $Na_2O{\cdot}2SiO_2$ glass in $Sr_{0.55}Na_{0.45}SiO_{2.775}$ and confirms the absence of Na doping in $SrSiO_3$ suggested before.[11–14,18,20]

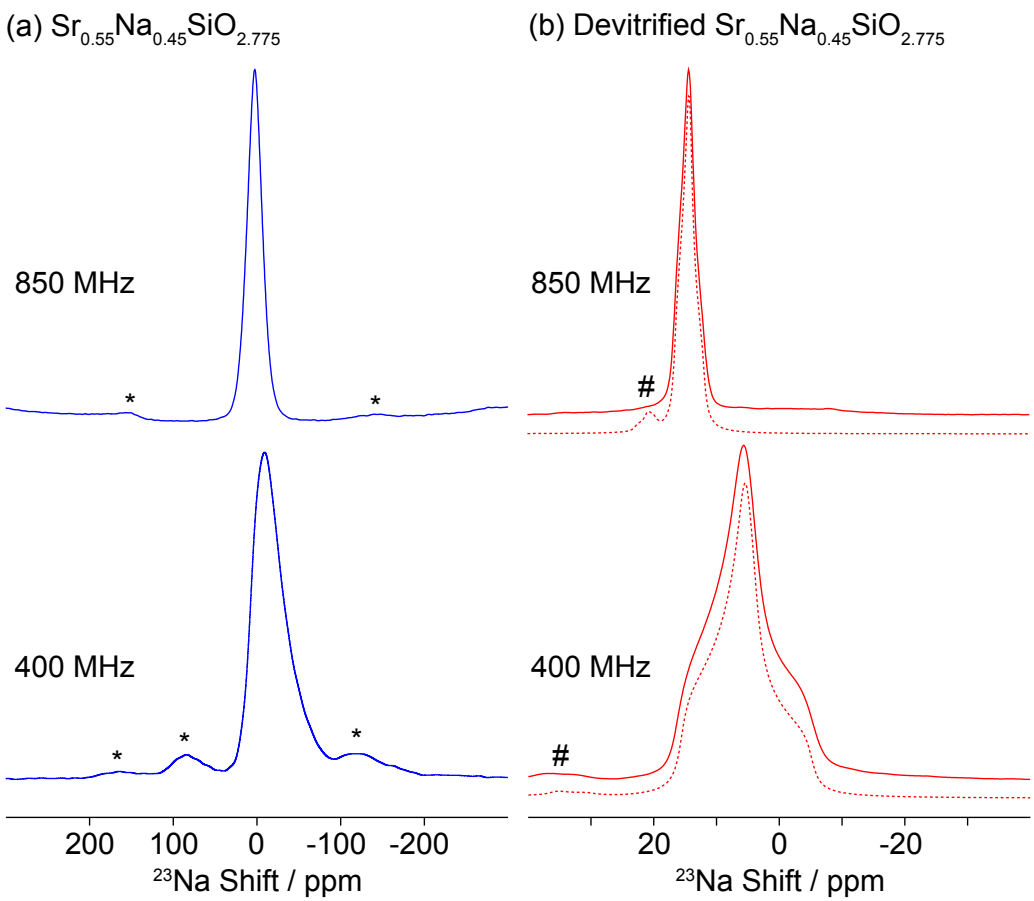

Figure 3. ^{23}Na MAS NMR spectra of (a) $Sr_{0.55}Na_{0.45}SiO_{2.775}$ and (b) devitrified $Sr_{0.55}Na_{0.45}SiO_{2.775}$ obtained at 9.4 and 20 T. Stars (*) and dash (#) indicate spinning sidebands and the outer satellite transition. Dashed lines represent the line shape simulation using the known NMR parameters for α-$Na_2Si_2O_5$ (isotropic chemical shift $\delta_{iso,cs}$ = 17.4 ppm, quadrupolar coupling constant C_Q = 1.82 MHz and asymmetry parameter η_Q = 1.0).[38] Note that these line shapes are offset from $\delta_{iso,cs}$ by the isotropic second-order quadrupolar shift $\delta_{iso,Q}$ ($\delta_{iso,Q}$ = 9.9 ppm and 2.2 ppm at 9.4 and 20 T, respectively) which varies inversely with the square of the strength of the magnetic field.[59]

Figure S1 presents the ^{17}O MAS NMR spectra ^{17}O enriched devitrified $Sr_{0.55}Na_{0.45}SiO_{2.775}$ (prepared by gas solid exchange with ^{17}O enriched O_2 gas)[60] and reveals a

range of broad signals between 75 and – 150 ppm (at 9.4 T) along with a weak low field signal around 94 ppm. Hu *et al.*[32] assigned the high field NMR signals (from 75 to – 150 ppm) to an amorphous $Na_2Si_2O_5$ phase, however these resonances undoubtedly appear at the shifts anticipated for all three oxygen sites expected in α-$Na_2Si_2O_5$[36] as Figure S1 demonstrates. The low field 94 ppm signals correspond very well with the position of the non-bridging oxygens O1 and O2 in α-$SrSiO_3$ and we note that the NMR signal of the bridging oxygen O3 in α-$SrSiO_3$ overlaps with the ones of α-$Na_2Si_2O_5$.

Na ion mobility: ^{23}Na NMR spectra line shape analysis

The room temperature ^{23}Na static NMR spectra of $Sr_{0.55}Na_{0.45}SiO_{2.775}$ is asymmetrically broadened (Figure 4a) as observed before[20] and corresponds to the amorphous $Na_2O{\cdot}2SiO_2$ glassy phase. Upon increasing the sample temperature to approximately 340 °C (using a standard solid-state NMR probe and N_2 gas as heat carrier), the ^{23}Na NMR lines narrow and yield a symmetric NMR line shape centred at – 21 ppm (Figures 4), in agreement with previous initial experimental work on $Sr_{0.6}Na_{0.4}SiO_{2.8}$,[20] as well as $Na_2O{\cdot}2SiO_2$ and $K_2O{\cdot}2SiO_2$ disilicates,[23] and confirmed computationaly,[19] which demonstrate that the $Na_2O{\cdot}2SiO_2$ glass is a fast Na ion conductor. The temperature evolution of the ^{23}Na line width ν and peak maxima position δ_{max} have been plotted in Figure 5 to give an overall indication of the line narrowing and change in δ_{max} with temperature, however the full analysis of the change in quadrupolar line shape with temperature results from a complex combination of 2nd order effects and dynamical shifts which are beyond the scope of this work.

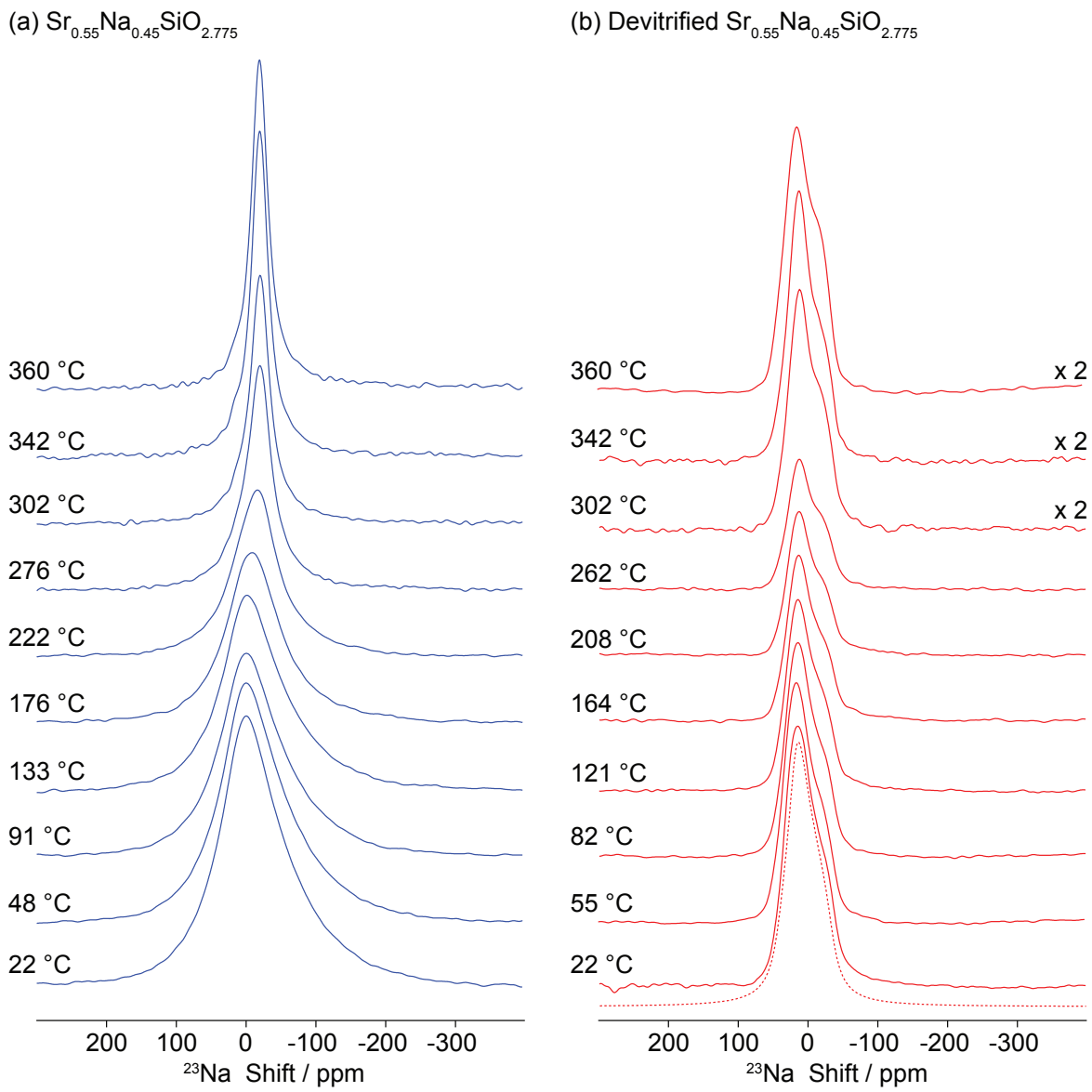

Figure 4. Representative high temperature ^{23}Na static NMR spectra of (a) $Sr_{0.55}Na_{0.45}SiO_{2.775}$ and (b) devitrified $Sr_{0.55}Na_{0.45}SiO_{2.775}$ obtained at 9.4 T on a standard NMR probe. The horizontal scaling factors are given on the right hand side of the spectra. Dashed lines represent line shape simulation using the NMR parameters of α-$Na_2Si_2O_5$.[38]

Unlike $Sr_{0.55}Na_{0.45}SiO_{2.775}$, the ^{23}Na static NMR line shape of the devitrified $Sr_{0.55}Na_{0.45}SiO_{2.775}$ material (Figure 4b) remains broad and is virtually unchanged (Figure 5a) as the temperature is increased to 360 °C, the integral of the spectra decreasing due to unfavourable Boltzmann distribution at high temperature. The lack of change in line shape is a clear indication

of the absence of Na ion dynamics and poor Na ion mobility as expected in α-$Na_2Si_2O_5$ and as determined by both its low conductivity[16] and the small atomic displacements computed by *ab initio* molecular dynamics simulation.[19]

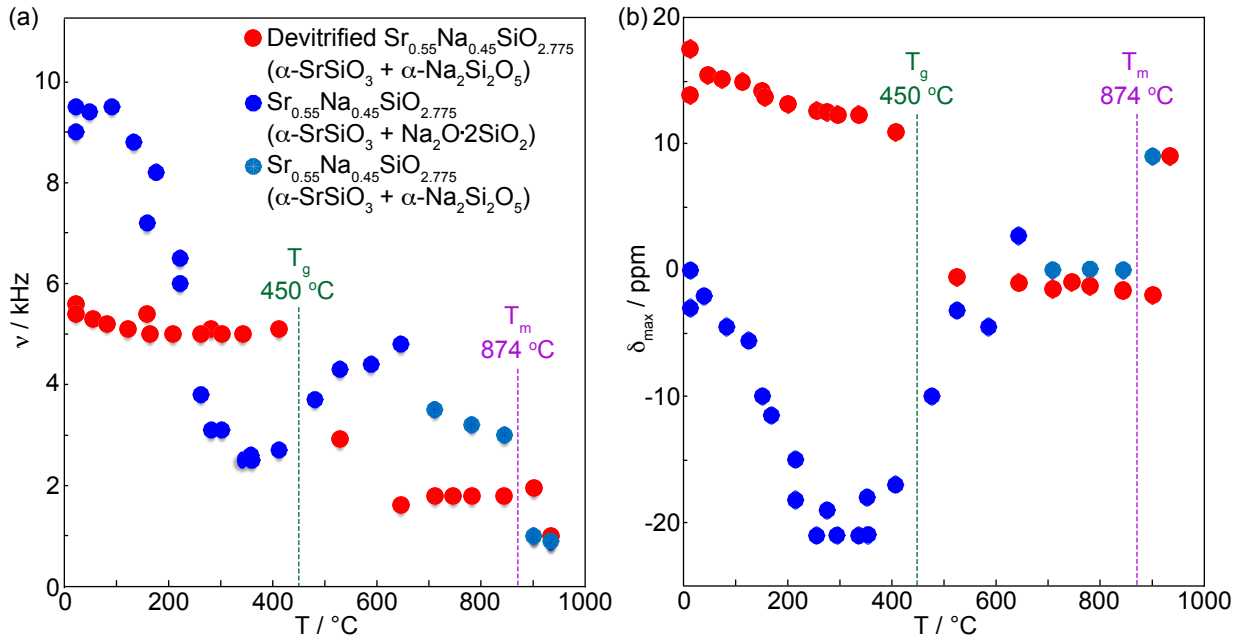

Figure 5. Temperature dependence of the (a) ^{23}Na NMR central transition line width ν (taken as full width at half-maximum) and (b) ^{23}Na peak position maxima δ_{max} of $Sr_{0.55}Na_{0.45}SiO_{2.775}$ (blue circles) and devitrified $Sr_{0.55}Na_{0.45}SiO_{2.775}$ (red circles) materials. Data were measured at a Larmor frequency of ν_0 = 105.8 MHz. The glass transition temperature T_g of $Na_2O{\cdot}2SiO_2$ glass (450 °C) and the melting point T_m of crystalline α-$Na_2Si_2O_5$ phase (874 °C) are given in the figure.

Additional high temperature static NMR experiments were performed on both $Sr_{0.55}Na_{0.45}SiO_{2.775}$ materials on a static NMR probe and a homemade CO_2 laser (λ = 10.6 μm, 250 W) heating system developed in Orléans (CNRS – CEMHTI)[48,49] to probe further the Na diffusion and *in situ* crystallisation behaviours (Figure 6). The width of ^{23}Na static NMR spectra of $Sr_{0.55}Na_{0.45}SiO_{2.775}$ (Figure 6a) decreases from room temperature to 358 – 412 °C then

broadens significantly at 529 °C. This broadening is due to a phase transition and the crystallisation of the amorphous $Na_2O{\cdot}2SiO_2$ glassy phase into crystalline α-$Na_2Si_2O_5$, a process that was surprisingly found to have multiple crystallisation phase transition temperatures T_c.[16] Crystallisation starts to occur at 490 °C and peaks at 550 and 650 °C as determined by differential scanning calorimetry (DSC)[16] and was observed in *in situ* high temperature XRD[16] and by ^{29}Si MAS NMR spectroscopy during the devitrification of $Na_2O{\cdot}2SiO_2$ glass.[42] These results are in contrast with the *in situ* high temperature ^{29}Si NMR study of pure $Na_2O{\cdot}2SiO_2$ glass[23] that shows the presence of a supercooled liquid phase up to about 200 °C above the T_g (450 °C) and no crystallisation of α-$Na_2Si_2O_5$. The presence of crystalline α-$SrSiO_3$ in $Sr_{0.55}Na_{0.45}SiO_{2.775}$ therefore dramatically changes the thermal behaviour of the $Na_2O{\cdot}2SiO_2$ glass present in the mixture by acting as seeds of the heterogeneous crystallisation.

As the temperature is increased further, the ^{23}Na line shape of $Sr_{0.55}Na_{0.45}SiO_{2.775}$ remains largely unchanged up to 845 °C with a slight shift of the resonances towards higher frequencies (see Figure 6b). At and above 901 °C, a much narrower Lorentzian line (full width at half maximum around 1 kHz) is observed indicative of a melted sample, in agreement with the known melting point T_m of α-$Na_2Si_2O_5$ (874 °C)[34] and visual inspection of the sample at room temperature after the high temperature NMR experiments. These experimental observations are also corroborated by *in situ* ^{23}Na two-dimensional quadrupole nutation NMR spectroscopy data that shows the non-selective central transition regime above T_m characteristic of liquid sample. Upon quenching of $Sr_{0.55}Na_{0.45}SiO_{2.775}$ from 934 °C to room temperature (in approximately 20 s) by turning off the laser suddenly, all ^{23}Na and ^{29}Si NMR data (Figures S3-4) and XRD pattern (Figure S2b) are consistent with the as prepared $Sr_{0.55}Na_{0.45}SiO_{2.775}$ showing the presence of crystalline α-$SrSiO_3$ and the amorphous $Na_2O{\cdot}2SiO_2$ glassy phase. The XRD data also shows that no reaction is observed between the BN crucible and the $Sr_{0.55}Na_{0.45}SiO_{2.775}$ phase under the reductive condition used with the laser NMR probe.

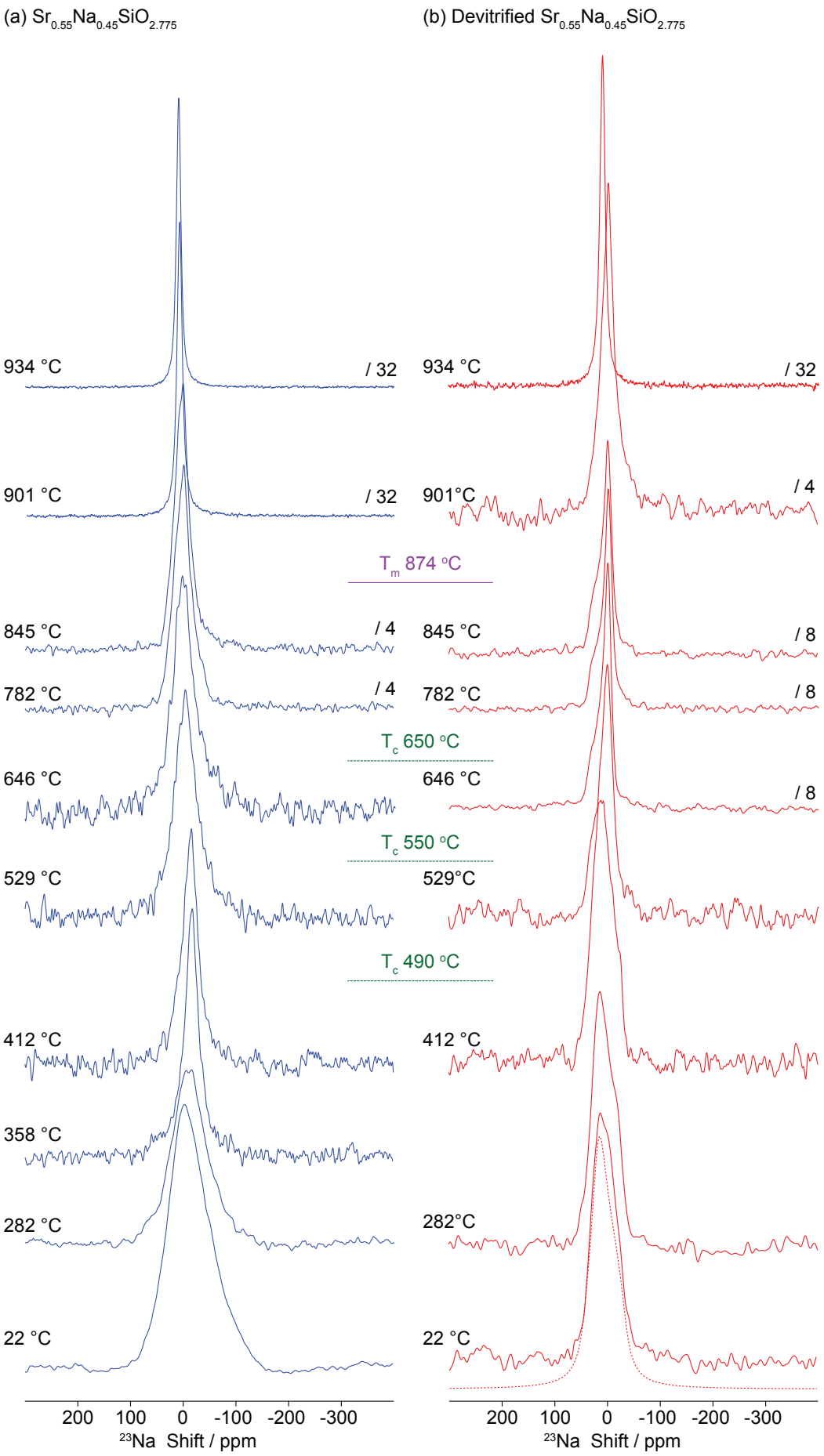
(a) $Sr_{0.55}Na_{0.45}SiO_{2.775}$
(b) Devitrified $Sr_{0.55}Na_{0.45}SiO_{2.775}$
934 °C
/ 32
901 °C
/ 32
T_m 874 °C
845 °C
/ 4
782 °C
/ 4
T_c 650 °C
646 °C
T_c 550 °C
529 °C
T_c 490 °C
412 °C
358 °C
282 °C
22 °C
934 °C
/ 32
901°C
/ 4
845 °C
/ 8
782 °C
/ 8
646 °C
/ 8
529°C
412 °C
282°C
22 °C
200 100 0 -100 -200 -300
^{23}Na Shift / ppm
200 100 0 -100 -200 -300
^{23}Na Shift / ppm

Figure 6. Representative very high temperature ^{23}Na static NMR spectra of (a) $Sr_{0.55}Na_{0.45}SiO_{2.775}$ and (b) devitrified $Sr_{0.55}Na_{0.45}SiO_{2.775}$ obtained at 9.4 T on a static laser NMR probe.[48,49] In (a), 4 times more transients were acquired for the ^{23}Na NMR data collected at and above 782 °C. In (b), 8 times more transients were acquired for the ^{23}Na NMR data collected at and above 649 °C. ^{23}Na spectra at and above 901 °C were obtained with a $\pi/2$ pulse length of 26 μs under the non-selective central transition regime (except at 901 °C in (b)). The crystallisation phase transition temperatures T_c of 490, 550 and 650 °C and the melting point T_m of 874 °C of α-$Na_2Si_2O_5$ are given in the figure. The horizontal scaling factors are given on the right hand side of the spectra. Dashed lines represent line shape simulation using the NMR parameters of α-$Na_2Si_2O_5$[38].

The ^{23}Na static NMR spectra of devitrified $Sr_{0.55}Na_{0.45}SiO_{2.775}$ given in Figure 6b is unchanged up to heating at 412 °C. Above this temperature, a change in line shape is observed. The change may be associated with some Na dynamics in α-$Na_2Si_2O_5$, or, even more likely, additional phase transitions in α-$Na_2Si_2O_5$, given the existence of a α_{III}-$Na_2Si_2O_5$ phase below 678 °C, α_{II}-$Na_2Si_2O_5$ between 678 and 707 °C, and α_{I}-$Na_2Si_2O_5$ above 707 °C, corresponding to small distortions of the SiO_4 groups.[33] Further heating of the devitrified $Sr_{0.55}Na_{0.45}SiO_{2.775}$ sample to 934 °C yields significant line narrowing of the ^{23}Na NMR spectrum, a Lorentzian line shape and a non-selective central transition regime, all consistent with melting of α-$Na_2Si_2O_5$ (T_m of 874 °C). Melting should have happened at the quoted static laser temperature of 901 °C (first temperature recorded above T_m), however the estimated probe temperature accuracy is around 30 °C in this high temperature range (see Experimental Section),[48,49] explaining the slight discrepancy. Additionally, it is likely that the rate of crystallisation is slow or that the T_m of α-$Na_2Si_2O_5$ in the presence of solid α-$SrSiO_3$ differs from the one of pure α-$Na_2Si_2O_5$.[33]

Quenching of the devitrified $Sr_{0.55}Na_{0.45}SiO_{2.775}$ melt from 934 °C to room temperature largely regenerates the as prepared $Sr_{0.55}Na_{0.45}SiO_{2.775}$ phase with crystalline α-$SrSiO_3$ and amorphous $Na_2O{\cdot}2SiO_2$ glassy phase detected by $^{23}Na/^{29}Si$ NMR and XRD (Figures S2c, S3-4). More specifically, the ^{29}Si MAS NMR spectrum (Figure S4) displays the sharp resonance at – 84.8 ppm associated with α-$SrSiO_3$ and a broad resonance consistent with an amorphous phase, and the absence of the sharp signal at – 94.3 ppm associated with α-$Na_2Si_2O_5$ (Figure 2) in agreement with the XRD pattern (Figure S2c) only revealing α-$SrSiO_3$ as the crystalline phase. The ^{23}Na static NMR spectrum (Figure S3) of this quenched material also shows a broad and featureless asymmetric peak rather than the second-order line shape of α-$Na_2Si_2O_5$ (Figures 6 and 8).

Comparison between the ^{23}Na static NMR spectra of both melts at 934 °C (Figure S5) obtained from the as prepared and devitrified $Sr_{0.55}Na_{0.45}SiO_{2.775}$ materials shows very good overlap, confirming that the only Na-containing compound in the molten state is liquid $Na_2Si_2O_5$.

Na ion mobility: ^{23}Na spin lattice relaxation rates

Probing dynamics and ionic motion could also be achieved from measuring the T_1^{-1} and/or $T_{1\rho}^{-1}$ rates and yield correlation times on the order of the Larmor frequency (~ 10^8 Hz) and spin lock frequency (~ 10^3 Hz).[61,62] The determination of the T_1^{-1} and/or $T_{1\rho}^{-1}$ rates has, for example, enabled the understanding of the Li ion diffusion processes and its quantification (jump rates, activation energies) in a range of fast lithium ion conductors using ^7Li NMR.[45,63–66] A similar approach is used here with ^{23}Na NMR to shed the light on the sodium dynamics in both $Sr_{0.55}Na_{0.45}SiO_{2.775}$ and devitrified $Sr_{0.55}Na_{0.45}SiO_{2.775}$ and to obtain quantitative information on the sodium mobility over a range of time scales and up to the melting point of $Na_2Si_2O_5$ (874 °C). The results complement the preliminary ^{23}Na T_1^{-1} investigation recently reported on $Sr_{0.6}Na_{0.4}SiO_{2.8}$ that were limited to temperatures from RT to 150 °C.[20] Figure 7 plots the

variable temperature ^{23}Na T_1^{-1} and $T_{1\rho}^{-1}$ rates of $Sr_{0.55}Na_{0.45}SiO_{2.775}$ from room temperature to 934 °C, above the melting point of the Na-containing phase α-$Na_2Si_2O_5$. As the temperature is increased from room temperature to approximately the first crystallization temperature T_c of the $Na_2O{\cdot}2SiO_2$ glassy phase (490 °C), the T_1^{-1} and $T_{1\rho}^{-1}$ values increased, indicating a slow motional regime (characterised by $2\pi\nu_0\tau_c >> 1$ and $2\pi\nu_1\tau_c >> 1$, respectively where ν_0, ν_1 and τ_c are the ^{23}Na Larmor frequency, the spin lock frequency and the correlation times of the motion)[61,62] and that the $T_{1(\rho)}^{-1}$ rates are sensitive to local site-to-site hopping. The data clearly follows an Arrhenius behaviour highlighting that the relaxation data indeed probes a thermally activated process. Activation energy values for the short range Na diffusion process of 28 ± 2 kJ.mol^{-1} (from T_1^{-1}) and ~ 22 ± 2 kJ.mol^{-1} (from $T_{1\rho}^{-1}$ above 160 °C) could be extracted.

Upon increasing the temperature further across the various T_c (490 – 650 °C) of the $Na_2O{\cdot}2SiO_2$ glass, a short and a long T_1 (plotted as light and dark blue in Figure 12, respectively) are required to fit the ^{23}Na saturation recovery experiments (see Experimental Section for details) of $Sr_{0.55}Na_{0.45}SiO_{2.77}$. The need for two T_1 values reflects a transition region with the onset of crystallisation of $Na_2O{\cdot}2SiO_2$ (short T_1) and the additional presence of the α-$Na_2Si_2O_5$ phase (long T_1) in $Sr_{0.55}Na_{0.45}SiO_{2.775}$. A single $T_{1\rho}$ value fits accurately the ^{23}Na spin lock experiments, however it is likely that the value obtained is an averaged $T_{1\rho}$ and echoes the fact that both $Na_2O{\cdot}2SiO_2$ glass and crystalline α-$Na_2Si_2O_5$ phases exist in $Sr_{0.55}Na_{0.45}SiO_{2.775}$ at these temperatures. The long ^{23}Na T_1^{-1} values (dark blue) start to level off (as observed around the T_g of the $Na_2O{\cdot}2SiO_2$ glass)[23] and a change in activation is observed (estimated to ~ 10 ± 3 kJ.mol^{-1}) in the 490 – 650 °C temperature range. Meanwhile the short ^{23}Na T_1^{-1} values (light blue) are of the same order of magnitude than for α-$Na_2Si_2O_5$ in devitrified $Sr_{0.55}Na_{0.45}SiO_{2.775}$ (red in Figure 7 - see below). Above 490 – 650 °C, α-$Na_2Si_2O_5$ is the only Na-containing phase and an Arrhenius plot of ^{23}Na T_1^{-1} from 650 °C to ~ T_m (874 °C) yields a large activation value of 123 ± 9 kJ.mol^{-1} (and similar to the one obtained for α-$Na_2Si_2O_5$ in devitrified

$Sr_{0.55}Na_{0.45}SiO_{2.775}$ - see below). Concomitantly, the measured ^{23}Na $T_{1\rho}^{-1}$ values decreases (green) and converges towards the ones obtained for α-$Na_2Si_2O_5$ (red/orange).

We note that the apparent $T_{1(\rho)}^{-1}$ maxima observed here around 490 – 650 °C are not representative of the $2\pi\nu_0\tau_c \sim 1$ and $2\pi\nu_1\tau_c \sim 0.5$ conditions observed in maxima of $T_{1(\rho)}^{-1}$ in Arrhenius plot of thermally activated processes.[61,62] Rather, the maxima correspond to changes occurring in $Sr_{0.55}Na_{0.45}SiO_{2.775}$ with temperature and the crystallisation of $Na_2O{\cdot}2SiO_2$ glass into α-$Na_2Si_2O_5$ which have short and long $T_{1(\rho)}$ values, respectively. Hence, the decrease of $T_{1\rho}^{-1}$ values with increasing temperature does not probe the fast motional regime (where the relationships $2\pi\nu_0\tau_c << 1$ and $2\pi\nu_1\tau_c << 1$ hold). This regime is not accessible here and therefore the $T_{1(\rho)}^{-1}$ rates do not access the long range Na diffusion in $Sr_{0.55}Na_{0.45}SiO_{2.775}$ and $Na_2O{\cdot}2SiO_2$ glass.

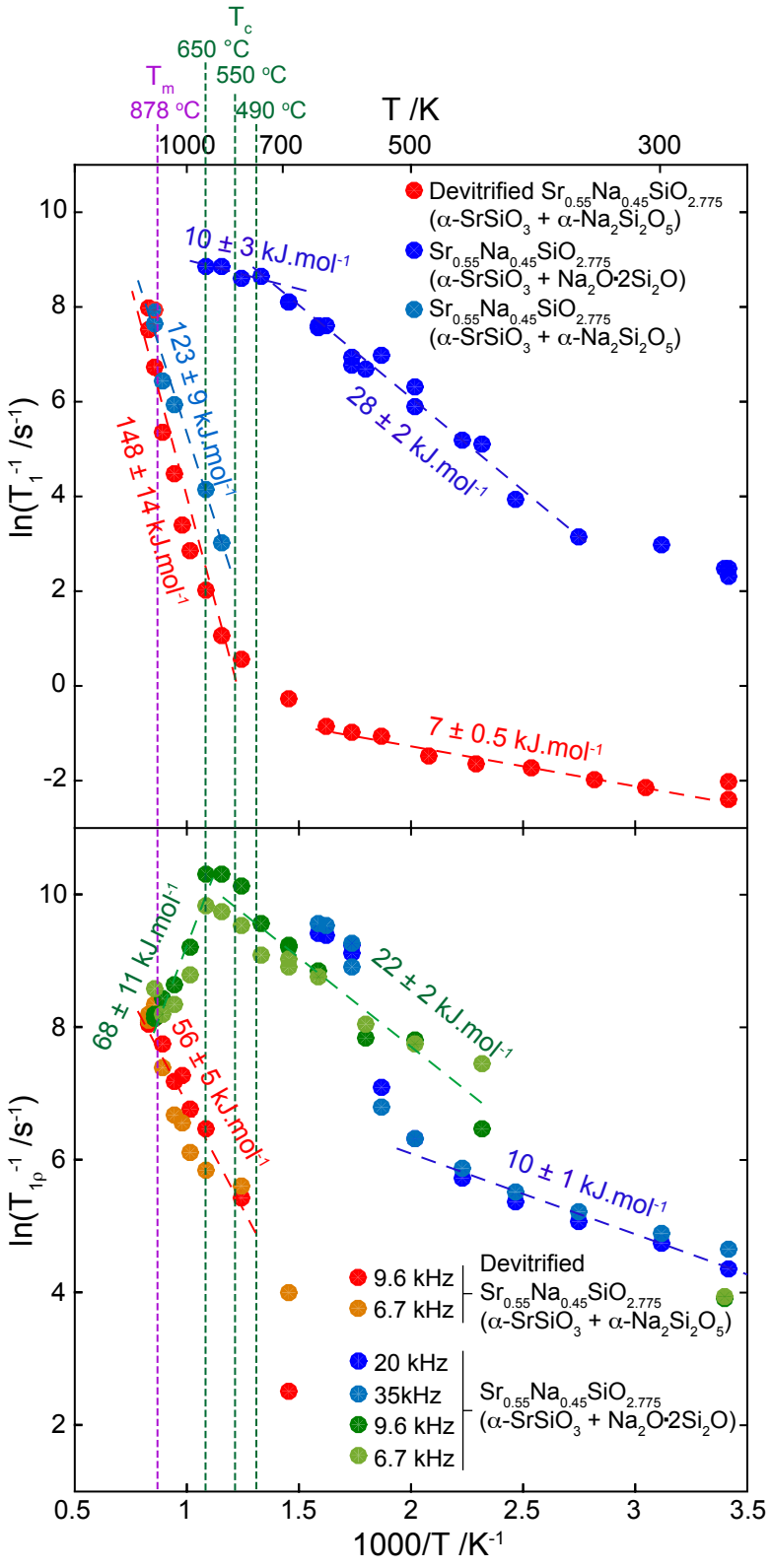

Figure 7. Arrhenius plot of the ^{23}Na spin lattice relaxation rates T_1^{-1} obtained in the laboratory frame at $\nu_0(^{23}Na)$ = 105.8 MHz and spin lattice relaxation rates $T_{1\rho}^{-1}$ obtained in the rotating frame at $\nu_1(^{23}Na)$ = 6.7, 9.6, 20 and 35 kHz. Data for $Sr_{0.55}Na_{0.45}SiO_{2.775}$ and devitrified

$Sr_{0.55}Na_{0.45}SiO_{2.775}$ are shown in blue/green and red/orange circles, respectively. The crystallisation phase transition temperatures T_c of $Na_2O{\cdot}2SiO_2$ (490, 550 and 650 °C) and the melting point T_m of crystalline α-$Na_2Si_2O_5$ (874 °C) are given in the figure. Error bars are smaller than symbol sizes.

Table 1 compares the activation energies obtained above with the ones obtained with ac impedance[2,10,14,16] and the previous ^{23}Na T_1^{-1} work.[20] A large range of activation energies (~ 17 – 75 kJ.mol^{-1}) has been obtained using ac impedance spectroscopy under comparable temperature range. These discrepancies probably reflect large changes in the actual sample composition of $Sr_{0.55}Na_{0.45}SiO_{2.77}$ and for example the presence or absence of crystalline $Na_2Si_2O_5$ and/or $Na_2O{\cdot}2SiO_2$ glass depending on the thermal history of the sample, both materials having very different Na ion conductivity properties.[16,19] The activation energy of 28 kJ.mol^{-1} obtained T_1^{-1} rates over the 22 – 490 °C temperature range compares well with the initial activation energy determined by ac impedance for $Sr_{0.55}Na_{0.45}SiO_{2.775}$ material (31 kJ.mol^{-1}),[10] although we note that this value was obtained at higher temperature and above the T_g of the $Na_2O{\cdot}2SiO_2$ glass (Table 1). The value of 28 kJ.mol^{-1} underestimates the ones obtained in a range of ac impedance studies (46 – 75 kJ.mol^{-1}) as often observed while monitoring ionic mobility using both techniques.[20,44,67] The lower activation energy obtained from NMR *versus* impedance is ascribed to the fact that a mobile ion has a greater probability to jump back to its original position rather than to a new site, and while ac impedance probes long range bulk mobility, the slow motional regime ($2\pi\nu_0\tau_c >> 1$) of the ^{23}Na NMR data detected here is being sensitive to local dynamics and short diffusion including unsuccessful jumps.[45,44]

Table 1. Comparison between the activation energies of sodium mobility in $Sr_{0.55}Na_{0.45}SiO_{2.775}$, $Na_2O{\cdot}2SiO_2$ glass, devitrified $Sr_{0.55}Na_{0.45}SiO_{2.775}$ and crystalline $Na_2Si_2O_5$ materials.

Material	E_a / kJ.mol^{-1}	Temperature range / °C	Method	Ref.
$Sr_{0.55}Na_{0.45}SiO_{2.775}$	75 ± 7	~ 350 – ~ 560	ac impedance	2
	46 ± 7	~ 560 – ~ 940		2
	31	450 – 680		10
	72	~ 280 – ~ 640		14
	~ 34	400 – 600		16
	23 ± 3	~ 22 – 150	^{23}Na NMR T_1^{-1}	20
	28 ± 2	22 – 490		This work
	~ 22 ± 2	22 – 650	^{23}Na NMR $T_{1\rho}^{-1}$	This work
$Na_2O{\cdot}2SiO_2$ glass	63 – 84	~ 100 – ~ 450	^{22}Na/^{24}Na tracer diffusion and electrical conductivity	26
	67	–	ac impedance	27
	72	~ 280 – ~ 460	^{22}Na tracer diffusion	28,29 a
	116	~ 460 – ~ 540		29
	67 ± 5	~ 530 – ~ 1100	^{23}Na NMR T_1^{-1}	23
	54 ± 2	1273 – 2273	molecular dynamics	30
	16	300 – 450	*ab* initio molecular dynamics	19
	29	450 – 700		19
	~ 67 ± 10	400 – ~ 500	ac impedance	16
Devitrified $Sr_{0.55}Na_{0.45}SiO_{2.775}$	7 ± 0.5	22 – 350	^{23}Na NMR T_1^{-1}	This work
	123 – 148 ± 14	550 – 830		This work
	~ 56 ± 5	490 – 830	^{23}Na NMR $T_{1\rho}^{-1}$	This work
Crystalline $Na_2Si_2O_5$	~ 42	400 – 650	ac impedance	16 b
	114 – 208	996 – 1146	*ab* initio molecular dynamics	19

[a] $Na_2O{\cdot}2SiO_2$ glass sample obtained from slow cooling from 475 °C (above T_g) to room temperature and may be partially crystalline.[28] [b] Probably the α-$Na_2Si_2O_5$ phase although not stated.

The activation energy value determined above from ^{23}Na T_1^{-1} relaxation data should also be compared with the values available in the literature for pure $Na_2O{\cdot}2SiO_2$. The activation energies for Na diffusion obtained below T_g using a range of experimental approaches (^{22}Na/^{24}Na tracer diffusion,[26,28,29] electrical conductivity,[26] ac impedance[16,27] and ^{23}Na NMR T_1^{-1} data[23]) are in relatively good agreement with each other (63 – 84 kJ.mol^{-1}, see Table 1). In particular that the value obtained from ^{23}Na NMR T_1^{-1} data[23] (67 ± 5 kJ.mol^{-1})[23] fits well into this range. However, we also note that a more recent *ab initio* molecular dynamics study deviates significantly from these observations (with activation energies of 16 and 29 kJ.mol^{-1}

between below and above T_g, respectively) and is most likely explained by the short simulation time used (40 ps) for the mean square displacement and the relative small size of the cell used (144 atoms).[11] The shorter Na^+ diffusion activation energies derived here for $Sr_{0.55}Na_{0.45}SiO_{2.775}$ are therefore much smaller than the ones experimentally obtained for pure $Na_2O{\cdot}2SiO_2$ glass, indicating that the presence of crystalline α-$SrSiO_3$ dramatically changes the Na^+ diffusion behaviour of the $Na_2O{\cdot}2SiO_2$ glass.

Figure 7 also plots the behaviour of T_1^{-1} rates versus temperature in the devitrified $Sr_{0.55}Na_{0.45}SiO_{2.775}$. As expected the T_1 values in this material are much longer (hence short T_1^{-1}) than the ones of as prepared $Sr_{0.55}Na_{0.45}SiO_{2.775}$ due to the presence of the crystalline α-$Na_2Si_2O_5$ phase. However, and in contrast to $Sr_{0.55}Na_{0.45}SiO_{2.775}$, at temperature below 450 °C, the T_1^{-1} rates of devitrified $Sr_{0.55}Na_{0.45}SiO_{2.775}$ are largely temperature independent and simply probe atomic vibration. Over the same temperature range, long $T_{1\rho}$ values are anticipated (longer than $T_{1\rho}$ ~ 82 ms obtained at 412 °C with ν_1 = 9.6 kHz) and could not be obtained due to limitation on the radio frequency capabilities of the liquid state NMR probe used in the high temperature setup.[48,49] Around 550 °C, a kink is clearly observed in the T_1^{-1} plot and both T_1^{-1} and $T_{1\rho}^{-1}$ rates increased quickly and follow Arrhenius behaviour from which the large activation energy values (148 ± 14 kJ.mol^{-1} and ~ 56 ± 5 kJ.mol^{-1}, respectively) demonstrate the poor Na ion mobility of the α-$Na_2Si_2O_5$ phase, supporting the recent *ab initio* molecular dynamics simulations on crystalline $Na_2Si_2O_5$.[11] Similar $T_{1(\rho)}$ values and activation energies (123 ± 9 kJ.mol^{-1} from T_1^{-1} and ~ 68 ± 11 kJ.mol^{-1} from $T_{1\rho}^{-1}$) were obtained in $Sr_{0.55}Na_{0.45}SiO_{2.775}$ above T_gs as the sample composition (α-$Na_2Si_2O_5$ and α-$SrSiO_3$) is identical to the one of devitrified $Sr_{0.55}Na_{0.45}SiO_{2.775}$.

Conclusions

In summary, the present multinuclear NMR study provides extensive evidence for the absence of Na doping in strontium silicate α-$SrSiO_3$ and the multiphasic nature of this $Sr_{0.55}Na_{0.45}SiO_{2.775}$ material. The NMR data indicate that this phase is made of a mixture of crystalline α-$SrSiO_3$, clearly identified by its narrow ^{29}Si linewidth and chemical shift, and an amorphous glassy phase of composition $Na_2O{\cdot}2SiO_2$, as evidenced by the detection of a single broad and featureless peak in both ^{23}Na and ^{29}Si NMR spectra. High temperature treatment of $Sr_{0.55}Na_{0.45}SiO_{2.775}$ at 800 °C, just below the melting point of its $Na_2O{\cdot}2SiO_2$ glass component (874 °C) followed by slow cooling to room temperature, devitrifies the $Na_2O{\cdot}2SiO_2$ glass. The XRD pattern of the resulting $Sr_{0.55}Na_{0.45}SiO_{2.775}$ phase indicates the presence of additional reflections to α-$SrSiO_3$, which could be structurally refined to crystalline α-$Na_2Si_2O_5$. Comparison between all the ^{17}O, ^{23}Na and ^{29}Si NMR data recorded on devitrified $Sr_{0.55}Na_{0.45}SiO_{2.775}$ with the ones known for this α-$Na_2Si_2O_5$ phase confirms its presence as the sole Na-containing material.

The high ionic conductivity in $Sr_{0.55}Na_{0.45}SiO_{2.775}$ originally attributed to the diffusion of oxide ions, and questioned quickly in the literature, is in fact due to the high sodium ion mobility observed in the $Na_2O{\cdot}2SiO_2$ glass. Extensive variable temperature ^{23}Na NMR experiments from room temperature to below the T_g of the $Na_2O{\cdot}2SiO_2$ glass (450 °C) reveals a clear line narrowing of the ^{23}Na line shape, resulting from the mobility of sodium ions, and an evident temperature dependency of the spin lattice relaxation rates $T_{1(\rho)}^{-1}$ corresponding to a thermally activated diffusion process with an activation energy in the 22 – 28 $kJ.mol^{-1}$ range. The same ^{23}Na NMR experiments carried out on devitrified $Sr_{0.55}Na_{0.45}SiO_{2.775}$ distinctively showed the absence of sodium ion transport in crystalline α-$Na_2Si_2O_5$ illustrated by the limited effect of temperature on the ^{23}Na line widths and spin lattice relaxation rates $T_{1(\rho)}^{-1}$. These observations are key findings which explain the large difference in the Na^+ ion conductivities and activation

energies reported for $Sr_{0.55}Na_{0.45}SiO_{2.775}$ and are due to large difference in sample composition (presence and/or absence of $Na_2O{\cdot}2SiO_2$ glass and crystalline α-$Na_2Si_2O_5$) and thermal history of the sample.

The experimental work presented here addresses the existing debate regarding the nature of the charge carrier in sodium strontium silicates by confirming the existence of fast sodium transport in an amorphous glassy $Na_2O{\cdot}2SiO_2$ component of the sample. These results highlight some potential materials issues with alkali metal substitution strategies for high temperature inorganic solid state electrolytes. However, we hope it will also highlight further the potential for using non crystalline solids as fast ionic transport.[68]

Associated Content

Supporting Information

The Supporting Information is available free of charge on the ACS Publications website. Additional ^{17}O, ^{23}Na, ^{29}Si NMR spectra and XRD patterns.

Author Information

Corresponding Author

Email: rbayliss@uic.edu (R.D.B.); frederic.blanc@liverpool.ac.uk (F.B.)

Notes

The authors declare no competing interest.

Acknowledgements

KKI thanks the EPSRC for a Doctoral Training Studentship. FB thanks SFTC for a "Futures Early Career Award" and the University of Liverpool for funding. We thank Colin Greaves, John A. Kilner and Stephen S. Skinner for helpful discussions during this project. The UK 850 MHz solid-state NMR Facility used in this research was funded by EPSRC and BBSRC, as well as the University of Warwick including via part funding through Birmingham Science City

Advanced Materials Projects 1 and 2 supported by Advantage West Midlands (AWM) and the European Regional Development Fund (ERDF).

References

(1) Singh, P.; Goodenough, J. B. $Sr_{1-x}K_xSi_{1-y}Ge_yO_{3-0.5x}$: A New Family of Superior Oxide-Ion Conductors. *Energy Environ. Sci.* **2012**, *5*, 9626–9631.

(2) Singh, P.; Goodenough, J. B. Monoclinic $Sr_{1-x}Na_xSiO_{3-0.5x}$: New Superior Oxide Ion Electrolytes. *J. Am. Chem. Soc.* **2013**, *135*, 10149–10154.

(3) Thangadurai, V.; Weppner, W. $Li_6ALa_2Ta_2O_{12}$ (A = Sr, Ba): Novel Garnet-Like Oxides for Fast Lithium Ion Conduction. *Adv. Funct. Mater.* **2005**, *15*, 107–112.

(4) Li, M.; Pietrowski, M. J.; De Souza, R. A.; Zhang, H.; Reaney, I. M.; Cook, S. N.; Kilner, J. A.; Sinclair, D. C. A Family of Oxide Ion Conductors Based on the Ferroelectric Perovskite $Na_{0.5}Bi_{0.5}TiO_3$. *Nat. Mater.* **2014**, *13*, 31–35.

(5) Xu, J.; Wang, X.; Fu, H.; Brown, C. M.; Jing, X.; Liao, F.; Lu, F.; Li, X.; Kuang, X.; Wu, M. Solid-State ^{29}Si NMR and Neutron-Diffraction Studies of $Sr_{0.7}K_{0.3}SiO_{2.85}$ Oxide Ion Conductors. *Inorg. Chem.* **2014**, *53*, 6962–6968.

(6) Martinez-Coronado, R.; Singh, P.; Alonso-Alonso, J.; Goodenough, J. B. Structural Investigation of the Oxide-Ion Electrolyte with $SrMO_3$ (M = Si/Ge) Structure. *J. Mater. Chem. A* **2014**, *2*, 4355–4360.

(7) Kilner, J. A. Fast Anion Transport in Solids. *Solid State Ionics* **1983**, *8*, 201–207.

(8) Kilner, J. A. Fast Oxygen Transport in Acceptor Doped Oxides. *Solid State Ionics* **2000**, *129*, 13–23.

(9) Manning, P. S.; Sirman, J. D.; De Souza, R. A.; Kilner, J. A. The Kinetics of Oxygen Transport in 9.5 Mol % Single Crystal Yttria Stabilised Zirconia. *Solid State Ionics* **1997**, *100*, 1–10.

(10) Wei, T.; Singh, P.; Gong, Y.; Goodenough, J. B.; Huang, Y.; Huang, K. $Sr_{3-3x}Na_{3x}Si_3O_{9-1.5x}$ (x = 0.45) as a Superior Solid Oxide-Ion Electrolyte for Intermediate Temperature-Solid Oxide Fuel Cells. *Energy Environ. Sci.* **2014**, *7*, 1680–1684.

(11) Bayliss, R. D.; Cook, S. N.; Fearn, S.; Kilner, J. A.; Greaves, C.; Skinner, S. J. On the Oxide Ion Conductivity of Potassium Doped Strontium Silicates. *Energy Environ. Sci.* **2014**, *7*, 2999–3005.

(12) Evans, I. R.; Evans, J. S. O.; Davies, H. G.; Haworth, A. R.; Tate, M. L. On $Sr_{1-x}Na_xSiO_{3-0.5x}$ New Superior Fast Ion Conductors. *Chem. Mater.* **2014**, *26*, 5187–5189.

(13) Bayliss, R. D.; Cook, S. N.; Scanlon, D. O.; Fearn, S.; Cabana, J.; Greaves, C.; Kilner, J. A.; Skinner, S. J. Understanding the Defect Chemistry of Alkali Metal Strontium Silicate Solid Solutions: Insights from Experiment and Theory. *J. Mater. Chem. A* **2014**, *2*, 17919–17924.

(14) Tealdi, C.; Malavasi, L.; Uda, I.; Ferrara, C.; Berbenni, V.; Mustarelli, P. Nature of Conductivity in $SrSiO_3$-Based Fast Ion Conductors. *Chem. Commun.* **2014**, *50*, 14732–14735.

(15) Fernández-Palacios, S.; Santos-Gómez, L. do.; Compana, J. M.; Porras-Vázquez, J. M.; Cabeza, A.; Marrero-López, D.; Losilla, E. R. Influence of the Synthesis Method on the Structure and Electrical Properties of $Sr_{1-x}K_xGeO_{3-x/2}$. *Ceram. Int.* **2015**, *41*, 6542–6551.

(16) Jee, Y.; Zhao, X.; Huang, K. On the Cause of Conductivity Degradation in Sodium Strontium Silicate Ionic Conductor. *Chem. Commun.* **2015**, *51*, 9640–9642.

(17) Jee, Y.; Zhao, X.; Lei, X.; Huang, K. Phase Relationship and Ionic Conductivity in Na-$SrSiO_3$ Ionic Conductor. *J. Am. Ceram. Soc.* **2016**, *99*, 324–331.

(18) Corley, J. P.; Cook, S. N.; Fearn, S.; Greaves, C.; Skinner, S. J.; Kilner, J. A.; Cabana, J.; Blanc, F.; Bayliss, R. D. Re-Evaluating the Defect Chemistry and Ion Mobility of "$Sr_{0.55}Na_{0.45}SiO_{2.775}$.", 20th International Conference on Solid State Ionics, Keystone

(CO), USA, June **2015**.

(19) Lei, X.; Jee, Y.; Huang, K. Amorphous $Na_2Si_2O_5$ as a Fast Na^+ Conductor: An Ab Initio Molecular Dynamics Simulation. *J. Mater. Chem. A* **2015**, *3*, 19920–19927.

(20) Peet, J. R.; Widdifield, C. M.; Apperley, D. C.; Hodgkinson, P.; Johnson, M. R.; Evans, I. R. Na^+ Mobility in Sodium Strontium Silicate Fast Ion Conductors. *Chem. Commun.* **2015**, *51*, 17163–17165.

(21) Lagaly, G.; Tufar, W.; Minihan, A.; Lovell, A. *Ùllman's Encyclopedia of Industrial Chemistry*; Wiley-VCH, 2000.

(22) Shelby, J. E. Property/Morphology Relations in Alkali Silicate Glasses. *J. Am. Ceram. Soc.* **1983**, *66*, 754–757.

(23) Liu, S. B.; Stebbins, J. F.; Schneider, E.; Pines, A. Diffusive Motion in Alkali Silicate Melts - An NMR-Study at High-Temperature. *Geochim. Cosmochim. Acta* **1988**, *52*, 527–538.

(24) Maekawa, H.; Yokokawa, T. Effects of Temperature on Silicate Melt Sructure: A High Temperature ^{29}Si NMR Study of $Na_2Si_2O_5$. *Geochim. Cosmochim. Acta* **1997**, *61*, 2569–2575.

(25) Gupta, Y. P.; King, T. B. Self-Diffusion of Sodium in Sodium Silicate Liquids. *Trans. Mettal. Soc. Aime* **1967**, *239*, 1701.

(26) Terai, R.; Hayami, R. Ionic Diffusion in Glasses. *J. Non. Cryst. Solids* **1975**, *18*, 217–264.

(27) Frischat, G. H. *Ionic Diffusion in Oxide Glasses*; Trans. Tech.: Aedermannsdorf, 1975.

(28) Kaps, C.; Voelksch, G. On the Interdiffusion of Ag^+ and Na^+ Ions in the Glass $Na_2O{\cdot}2SiO_2$ around the Glass Transition Temperature. *J. Non. Cryst. Solids* **1982**, *53*, 143–153.

(29) Kaps, C. On the Self-Diffusion of Na^+ Ions in the Glass $Na_2O{\cdot}2SiO_2$ around the Glass Transition Temperature. *J. Non. Cryst. Solids* **1984**, *65*, 189–192.

(30) Smith, W.; Greaves, G. N.; Gillan, M. J. Computer Simulation of Sodium Disilicate Glass. *J. Chem. Phys.* **1995**, *103*, 3091–3097.

(31) Isard, J. O. The Mixed Alkali Effect in Glass. *J. Non. Cryst. Solids* **1969**, *1*, 235–261.

(32) Chien, P.-H.; Jee, Y.; Huang, C.; Dervişoğlu, R.; Hung, I.; Gan, Z.; Huang, K.; Hu, Y.-Y. On the Origin of High Ionic Conductivity in Na-Doped $SrSiO_3$. *Chem. Sci.* **2016**, DOI: 10.1039/C5SC04270D

(33) Williams, J.; Glasser, F. P. Crystallisation of $Na_2O{\cdot}2SiO_2$-SiO_2 Glasses. *Phys. Chem. Glass* **1966**, *7*, 127.

(34) Kracek, F. C. The System Sodium Oxide-Silica. *J. Phys. Chem.* **1930**, *34*, 1583–1598.

(35) Pant, A. K.; Cruickshank, D. W. J. The Crystal Structure of α-$Na_2Si_2O_5$. *Acta Crystallogr. Sect. A* **1968**, *B24*, 13–19.

(36) Xue, X.; Stebbins, J. F.; Kanzaki, M. Correlations between ^{17}O NMR Parameters and Local Structure Around Oxygen in High Pressure Silicates - Implications for the Structure of Silicate Melts At High Pressure. *Am. Mineral.* **1994**, *79*, 31–42.

(37) Maekawa, H.; Florian, P.; Massiot, D.; Kiyono, H.; Nakamura, M. Effect of Alkali Metal Oxide on ^{17}O NMR Parameters and Si−O−Si Angles of Alkali Metal Disilicate Glasses. *J. Phys. Chem.* **1996**, *100*, 5525–5532.

(38) Heidemann, D.; Hubert, C.; Schwieger, W.; Grabner, P.; Bergk, K.-H.; Sarv, P. ^{29}Si Und ^{23}Na-Festkuerper-MAS-NMR-Untersuchungen an Modifikationen Des $Na_2Si_2O_5$. *Z. Anorg. Allg. Chem.* **1992**, *617*, 169–177.

(39) Xue, X.; Stebbins, J. F. ^{23}Na NMR Chemical Shifts and Local Na Coordination Environments in Silicate Crystals, Melts and Glasses. *Phys. Chem. Miner.* **1993**, *20*, 297–307.

(40) Koller, H.; Engelhardt, G.; Kentgens, A. P. M.; Sauer, J. ^{23}Na NMR Spectroscopy of Solids: Interpretation of Quadrupole Interaction Parameters and Chemical Shifts. *J. Phys.*

Chem. **1994**, *98*, 1544–1551.

(41) Engelhardt, G.; Michel, D. *High-Resolution Solid-State NMR of Silicates and Zeolites*; Wiley: New York, 1987.

(42) Mortuza, M. G.; Dupree, R.; Holland, D. Devitrification of Sodium Disilicate Glass: A NMR Study. *J. Mater. Sci.* **1998**, *33*, 3737–3740.

(43) Charpentier, T.; Ispas, S.; Profeta, M.; Mauri, F.; Pickard, C. J. First-Principles Calculation of ^{17}O, ^{29}Si, and ^{23}Na NMR Spectra of Sodium Silicate Crystals and Glasses. *J. Phys. Chem. B* **2004**, *108*, 4147–4161.

(44) Blanc, F.; Spencer, L.; Goward, G. R. Quadrupolar NMR of Ionic Conductors, Batteries, and Other Energy-Related Materials. *Encyclopedia of Magnetic Resonance*, 2011, DOI: 10.1002/9780470034590.emrstm1215.

(45) Wilkening, M.; Heitjans, P. From Micro to Macro: Access to Long-Range Li^+ Diffusion Parameters in Solids via Microscopic $^{6,7}Li$ Spin-Alignment Echo NMR Spectroscopy. *Chem. Phys. Chem.* **2012**, *13*, 53–65.

(46) Toby, B. H. EXPGUI, a Graphical User Interface for GSAS. *J. Appl. Cryst.* **2001**, *34*, 210–213.

(47) Larson, A. C.; Von Dreele, R. B. General Structure Analysis System (GSAS). *Los Alamos Natl. Lab. Rep.* **2000**, LAUR 86–748.

(48) Lacassagne, V.; Bessada, C.; Ollivier, B.; Massiot, D.; Florian, P.; Coutures, J. P. ^{27}Al, ^{23}Na, ^{19}F NMR Study of Cryolife at the Solid/liquid Transition. *C. R. Acad. Sci.* **1997**, *IIb*, 91–98.

(49) Lacassagne, V.; Bessada, C.; Florian, P.; Bouvet, S.; Ollivier, B.; Coutures, J.-P.; Massiot, D. Structure of High-Temperature $NaF-AlF_3-Al_2O_3$ Melts: A Multinuclear NMR Study. *J. Phys. Chem. B* **2002**, *106*, 1862–1868.

(50) Bielecki, A.; Burum, D. P. Temperature-Dependence of ^{207}Pb Mas Spectra of Solid Lead

Nitrate. An Accurate, Sensitive Thermometer for Variable-Temperature MAS. *J. Magn. Reson. Ser. A* **1995**, *116*, 215–220.

(51) Beckmann, P. A.; Dybowski, C. A Thermometer for Nonspinning Solid-State NMR Spectroscopy. *J. Magn. Reson.* **2000**, *146*, 379–380.

(52) Becker, K. D. Temperature Dependence of NMR Chemical Shifts in Cuprous Halides. *J. Chem. Phys.* **1978**, *68*, 3785–3793.

(53) Jingshi, W.; Namjun, K.; Stebbins, J. F. Temperature Calibration for High-Temperature MAS NMR to 913 K: ^{63}Cu MAS NMR of CuBr and CuI, and ^{23}Na MAS NMR of $NaNbO_3$. *Solid State Nucl. Magn. Reson.* **2011**, *40*, 45–50.

(54) Nishi, F. Strontium Metasilicate, $SrSiO_3$. *Acta Crystallogr. Sect. C-Crystal Struct. Commun.* **1997**, *53*, 534–536.

(55) Smith, K. A.; Kirkpatrick, R. J.; Oldfield, E.; Henderson, D. M. High-Resolution Silicon-29 Nuclear Magnetic Resonance Spectroscopic Study of Rock-Forming Silicates. *Am. Mineral.* **1983**, *68*, 1206–1215.

(56) Murdoch, J. B.; Stebbins, J. F.; Carmichael, I. S. E. High-Resolution ^{29}Si NMR Study of Silicate and Aluminosilicate Glasses: The Effect of Network-Modifying Cations. *Am. Mineral.* **1985**, *70*, 332–343.

(57) Xue, X. Y.; Stebbins, J. F.; Kanzaki, M.; McMillan, P. F.; Poe, B. Pressure-Induced Silicon Coordination and Tetrahedral Structural Changes in Alkali Oxide Silica Melts up to 12 GPa - NMR, Raman, and Infrared Spectroscopy. *Am. Mineral.* **1991**, *76*, 8–26.

(58) Massiot, D.; Fayon, F.; Capron, M.; King, I.; Le Calvé, S.; Alonso, B.; Durand, J.-O.; Bujoli, B.; Gan, Z.; Hoatson, G. Modelling One- and Two-Dimensional Solid-State NMR Spectra. *Magn. Reson. Chem.* **2002**, *40*, 70–76.

(59) Smith, M. E.; van Eck, E. R. H. Recent Advances in Experimental Solid State NMR Methodology for Half-Integer Spin Quadrupolar Nuclei. *Prog. Nucl. Magn. Reson.*

Spectrosc. **1999**, *34*, 159–201.

(60) Ashbrook, S. E.; Smith, M. E. Solid State ^{17}O NMR - an Introduction to the Background Principles and Applications to Inorganic Materials. *Chem. Soc. Rev.* **2006**, *35*, 718–735.

(61) Abragam, A. *Principles of Nuclear Magnetism*; Oxford University Press: Oxford, 1961.

(62) Steigel, A.; Spiess, H. W. *NMR Basic Principles and Progress*; Springer-Verlag: Berlin, 1978.

(63) Wilkening, M.; Küchler, W.; Heitjans, P. From Ultraslow to Fast Lithium Diffusion in the 2D Ion Conductor $Li_{0.7}TiS_2$ Probed Directly by Stimulated-Echo NMR and Nuclear Magnetic Relaxation. *Phys. Rev. Lett.* **2006**, *97*, 065901.

(64) Kuhn, A.; Sreeraj, P.; Poettgen, R.; Wiemhoefer, H.-D.; Wilkening, M.; Heitjans, P. Li Ion Diffusion in the Anode Material $Li_{12}Si_7$: Ultrafast Quasi-1D Diffusion and Two Distinct Fast 3D Jump Processes Separately Revealed by ^7Li NMR Relaxometry. *J. Am. Chem. Soc.* **2011**, *133*, 11018–11021.

(65) Kuhn, A.; Duppel, V.; Lotsch, B. V. Tetragonal $Li_{10}GeP_2S_{12}$ and Li_7GePS_8 – Exploring the Li Ion Dynamics in LGPS Li Electrolytes. *Energy Environ. Sci.* **2013**, *6*, 3548–3552.

(66) Epp, V.; Gun, O.; Deiseroth, H. J.; Wilkening, M. Highly Mobile Ions: Low-Temperature NMR Directly Probes Extremely Fast Li^+ Hopping Argyrodite-Type Li_6PS_5Br. *J. Phys. Chem. Lett.* **2013**, *4*, 2118–2123.

(67) Kim, N.; Hsieh, C. H.; Huang, H.; Prinz, F. B.; Stebbins, J. F. High Temperature ^{17}O MAS NMR Study Scandia and Yttria Stabilized of Calcia, Magnesia, Zirconia. *Solid State Ionics* **2007**, *178*, 1499–1506.

(68) Bachman, J. C.; Muy, S.; Grimaud, A.; Chang, H.-H.; Pour, N.; Lux, S. F.; Paschos, O.; Maglia, F.; Lupart, S.; Lamp, P.; *et al.* Inorganic Solid-State Electrolytes for Lithium Batteries: Mechanisms and Properties Governing Ion Conduction. *Chem. Rev.* **2016**, *116*, 140–162.

Table of Contents